



## Dual Port Disc Monopole Antenna for Wide-Band MIMO Based Wireless Applications

Journal:	<i>Microwave and Optical Technology Letters</i>
Manuscript ID	MOP-17-0550
Wiley - Manuscript type:	Research Article
Date Submitted by the Author:	23-Apr-2017
Complete List of Authors:	Nawaz, Haq; Sabanci University, Electronics Engineering Tekin, Ibrahim; Sabanci University, Telecommunications
Keywords:	Dual port antenna, Wide bandwidth, Orthogonal polarization, RF isolation

SCHOLARONE™  
Manuscripts

Review

# Dual Port Disc Monopole Antenna for Wide-Band MIMO Based Wireless Applications

Haq Nawaz and Ibrahim Tekin

Electronics Engineering, Sabanci University

34956, Istanbul, Turkey

e-mail: [hnawaz@sabanciuniv.edu](mailto:hnawaz@sabanciuniv.edu), [tekin@sabanciuniv.edu](mailto:tekin@sabanciuniv.edu)

Phone: +90 216 4839534, Fax: +90 216 4839550

**Abstract:** In this paper, design and implementation of a wide-band dual port monopole antenna based on single circular disc radiating element has been presented for Multi Input Multi Output (MIMO) configured 4G mobile and wireless communication systems. The proposed antenna uses a partial ground plane with two rectangular grooves which lie exactly below the respective  $50\Omega$  microstrip feeding lines in order to obtain enhanced antenna's impedance bandwidth of 2-6GHz. A circular cut with 14mm radius and centred at intersection of two partial rectangular ground planes is etched to reduce port to port RF coupling. The implemented dual port monopole antenna on 1.575mm thick RT/Duroid® 5880 substrate (with  $\epsilon=2.2$ , tangent loss =.001) provides more than 15dB RF interport isolation for antenna's 10dB impedance bandwidth of 2-6GHz with measured gain variations of 2-6dBi for each port excitation. In addition to interport isolation measurement for dual port antenna, the envelope correlation coefficient over the required frequency range has been calculated and plotted using  $S_{11}$ ,  $S_{22}$  and  $S_{21}$  measurement results to endorse the performance of dual port implemented antenna for diversity applications.

**Key words:** Dual port antenna, Wide bandwidth, Orthogonal polarization, RF isolation

## 1. Introduction

Wideband mobile and wireless communication systems with high data rate capacity along with reliable communication link performance are in great demand for current fast growing wireless applications [1]. Multiple Input Multiple Output (MIMO) technology improves the data throughput of wireless and mobile communication systems by deploying radio transceivers with multiple antennas to transmit and receive RF signals in rich scattered wireless environments [2-3]. MIMO techniques accomplish the task of improvement in data throughput and system capacity through spatially separated multiple wireless channels working at same carrier frequency (uncorrelated signals) and without additional transmit power requirements in Non Line of Sight (NLOS) communications [1],[4]. MIMO techniques are also very useful to improve the performance of wireless and mobile communication systems by minimizing the multi path propagation effect [5-6].

The MIMO antenna plays an important role to improve the overall performance of MIMO systems. Although, MIMO technology improves the capacity and reliability of wireless systems but the mutual coupling between multiple antennas degrades the obtainable MIMO performances due to increased signal correlation between multiple radio signals [7]. The coupling can be reduced by placing multiple antennas with large spatial displacements but it prevents the realization of compact transceiver [8]. The effect of mutual coupling can not be ignored in order to realize a compact MIMO transceiver where multiple antennas with minimum inter spacing are required to be fabricated on same substrate [1]. Realization of a compact MIMO antenna with required interport isolation is a challenging task [1].

The printed antennas are preferred for MIMO transceivers due to their ease of integration and low cost. For conventional compact MIMO transceivers, sufficiently separated multiple planar radiating elements are deployed and either isolation improvement techniques [9-19] or decoupling networks [20-21] are used to achieve required amount of interport

1  
2  
3 isolation for MIMO applications. For example, the antenna using two folded monopoles  
4 presented in [9] operates in 2.30-2.39 GHz frequency range and uses additional ground wall  
5 with connecting line to decrease the mutual coupling between antennas. A printed diversity  
6 monopole antenna for 2.4 GHz WLAN operation band is presented in [10]. It deploys T-  
7 shaped ground plane between two orthogonal linear monopoles for ports decoupling. A  
8 negative group delay based correlation reduction technique for closely spaced antennas  
9 technique has been proposed in [11] which reduces mutual coupling between antennas and  
10 also un-correlates the radiation characteristic of antennas. A compact MIMO antenna using  
11 two planar-monopole antenna elements has been presented in [12] for portable UWB  
12 applications. In this design, microstrip feed lines have been used to excite the two  
13 orthogonally placed antenna elements. Two long protruding ground stubs etched in ground  
14 plane improve antenna's impedance bandwidth and reduce the mutual coupling. A 2.4GHz  
15 compact MIMO structure has been presented in [13], which uses two different types of  
16 radiating elements. It uses one proximity coupled square ring patch antenna co-located with  
17 probe fed PIFA. Both radiators are designed to work at 2.4GHz WLAN frequency and high  
18 inter-port isolation (below 25 dB) is obtained through orthogonal polarization. In [14], a dual  
19 port planar canonical antenna is presented which uses folded slots as radiating  
20 elements. Coupling parasitic elements between canonical antennas have been used for field  
21 cancellation to improve the isolation. MIMO antennas with even number of ports can be  
22 designed by replicating this proposed dual port planar canonical antenna. A compact multiple-  
23 input multiple-output (MIMO) antenna with low correlation for UWB applications has been  
24 presented in [15]. The proposed structure is comprised of two identical radiating elements fed  
25 through 50 ohms microstrip lines and placed over half sized ground plane which is  
26 triangularly trimmed on two edges adjacent to radiating element to achieve better input  
27 impedance. The orthogonal placement of two antenna elements provides good interport  
28  
29  
30  
31  
32  
33  
34  
35  
36  
37  
38  
39  
40  
41  
42  
43  
44  
45  
46  
47  
48  
49  
50  
51  
52  
53  
54  
55  
56  
57  
58  
59  
60

1  
2  
3 isolation. The work in [16] presents a wideband isolation technique with neutralization lines  
4 for two crescent shaped printed monopole antennas placed very close to each other. The  
5 proposed antenna provides high isolation over 2.4-4.2GHz frequency band. Two antennas  
6 configuration, each comprised of two radiating elements has been presented in [17]. One  
7 configuration uses two parallel placed radiating element while the other one utilizes reverse  
8 parallel placement of antenna elements. Inverted T-shaped stubs have been used to obtain low  
9 port to port coupling over UWB frequency range. A novel neutralization technique based on  
10 two defected ground structures (a line slot and T-shaped slot etched on the ground plane) has  
11 been used in [18] to reduce the coupling between two UWB slot antennas. An ultra wideband  
12 MIMO antenna array has been presented in [19] to achieve 21dB isolation over 2.5–12 GHz  
13 frequency range by exploiting polarization diversity of two straight edged monopole radiator  
14 fed with arced feeding mechanism and placed over partial ground planes. Some antennas  
15 deploy external decoupling networks to suppress mutual coupling between elements and such  
16 decoupling networks are either based on circuit approach [20] or use lumped elements [21] to  
17 obtain improved interport isolation. For example, a circuit based technique has been used in  
18 [20] to increase the isolation between two strongly coupled antennas while a lumped elements  
19 technique has been presented in [21] to reduce the coupling between two closely packed  
20 antennas. These techniques may also be deployed for MIMO antennas.

21  
22 In contrast to above reviewed research works [9-21] where multiple antenna elements  
23 are incorporated in to one antenna design or etched on same substrate to realize a compact  
24 MIMO antenna, single antenna element with multiple RF isolated feeding ports can be used in  
25 more compact form for MIMO applications. Such configuration is termed as isolated mode  
26 antenna (iMAT) [22]. Such structures excite different propagating modes in antenna for  
27 feeding from each port to reduce mutual coupling between ports [23-27]. For example, a  
28 novel dual port, single element antenna for 4G MIMO terminals based on iMAT idea has  
29  
30  
31  
32  
33  
34  
35  
36  
37  
38  
39  
40  
41  
42  
43  
44  
45  
46  
47  
48  
49  
50  
51  
52  
53  
54  
55  
56  
57  
58  
59  
60

1  
2  
3 been proposed and analysed in [23]. The concept of iMAT antenna has also been used in [24]  
4  
5 for U-shaped single element antenna to obtain improved port to port isolation performance as  
6  
7 compared to compact two elements monopole antenna. A dual fed compact ultra-wideband  
8  
9 microstrip monopole antenna with reconfigurable polarisation capability has been presented  
10  
11 in [25] for cognitive radio systems where two orthogonal feeds using different transmission  
12  
13 line technology have been used to improve RF isolation between two ports. One port uses  
14  
15 50 $\Omega$  feed line using coplanar waveguide (CPW) structure while the other port excites the  
16  
17 radiating patch using 50 $\Omega$  Microstrip (MS) feed line. The proposed antenna provides more  
18  
19 than 25dB port to port isolation for 3.1 GHz to 10.6 GHz bandwidth based on a reflection  
20  
21 coefficient of less than -10 dB. A dual-polarized MIMO antenna proposed in [26] for indoor  
22  
23 wireless access point applications uses two perpendicular coplanar waveguide fed ports in  
24  
25 order to excite two orthogonally polarized modes. Implemented antenna structure utilizes  
26  
27 stepped cut at four corners (SCFC) technique which obtains required bandwidth by modifying  
28  
29 the shape of radiating patch. Implemented antenna on FR-4 substrate achieves around 15dB  
30  
31 interport isolation for 10dB impedance bandwidth of 900MHz to 2.7GHz. A 2.4GHz dual port  
32  
33 microstrip antenna which uses external loop in order to achieve around 75dB port to port peak  
34  
35 isolation has been presented in [27] for in band full duplex applications. Implemented antenna  
36  
37 achieves more than 40dB interport isolation in 50MHz bandwidth.  
38  
39  
40

41 Most of reported antenna works in literature as reviewed above are either narrow band  
42  
43 structures or focus on MIMO antennas for UWB applications with lower cut-off frequency of  
44  
45 3.1GHz. Such antenna structures are unable to support MIMO applications with operating  
46  
47 frequencies around 2.4GHz including 802.11b, 802.11g, 2.4GHz 802.11n, 2.5GHz WiMax  
48  
49 and LTE technology). In this work, dual port monopole antenna based on single circular disc  
50  
51 radiator has been designed and its parametric study has been carried out to obtain required  
52  
53 impedance bandwidth of 2-6GHz and more than 15dB interport RF isolation. The  
54  
55  
56  
57  
58  
59  
60

1  
2  
3 implemented antenna supports 2-6GHz MIMO applications including 2.4GHz operating  
4 frequency. As the obtainable bandwidth for single element based MIMO antennas depends  
5 upon many factors including feeding techniques and size of partial ground plane but the shape  
6 and size of single radiating element plays a critical role in this regard [28]. Thus, wideband  
7 planar single element should be selected as it could be potential wideband MIMO antenna  
8 when fed through multiple ports. In this work, we have selected circular planar radiating  
9 element as it provides better impedance bandwidth [29]. The optimized dual port antenna has  
10 been implemented on 1.575mm thick RT/Duroid® 5880 substrate to validate the simulation  
11 results. Measured transmission coefficient ( $S_{12}$  or  $S_{21}$ ) and calculated correlation coefficient  
12 have been used as two metrics to evaluate the interport RF isolation performance for intended  
13 impedance bandwidth of 2-6GHz for implemented dual port single element circular disc  
14 monopole antenna.  
15  
16  
17  
18  
19  
20  
21  
22  
23  
24  
25  
26  
27

28 The rest of this paper has been organised as follows: Section 2 provides the design,  
29 simulation, parametric optimization study and measured 10dB impedance bandwidth results  
30 for single port circular monopole antenna on which our proposed and implemented dual port  
31 monopole antenna is based on. Design and HFSS simulation for optimized matching and  
32 interport RF isolation along with implementation details of dual port monopole antenna based  
33 on single circular element are presented in section 3. Measured input impedance bandwidth  
34 for each port, port to port RF isolation and gain measurement results are discussed in section  
35 4. Calculated envelope correlation coefficient results using simulated and measured S-  
36 parameters for dual port antenna are discussed in same section. Finally, the paper is concluded  
37 in section 5.  
38  
39  
40  
41  
42  
43  
44  
45  
46  
47  
48  
49  
50

## 51 **2. Single port circular disc monopole antenna**

52 As our dual port monopole antenna is based on single radiating element so first of all a  
53 single port circular disc monopole antenna has been designed and its performance is evaluated  
54  
55  
56  
57  
58  
59  
60

in order to implement dual port antenna by adding second port to single port antenna and interport coupling has been suppressed by modifying the partial ground plane. The structure of single port circular disc monopole antenna is shown in Fig.1 where  $r$  and  $L_g$  represent the radius of circular disc and width of ground plane respectively. The optimized values of these two parameters are obtained through HFSS simulations in order to obtain required input impedance performance of antenna.

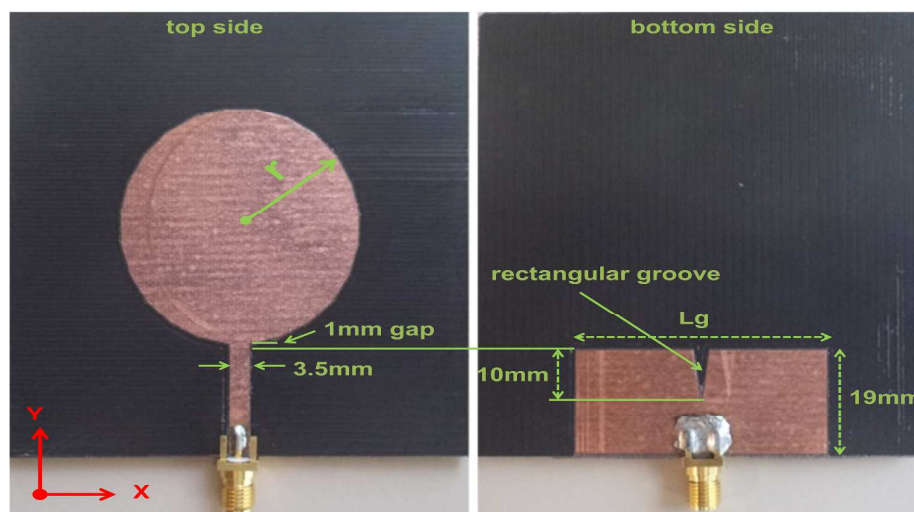


**Fig. 1.** Single port circular disc monopole antenna with rectangular groove in partial ground plane

Circular disc is excited through 3.5mm wide and 20mm ( $50\Omega$ ) long microstrip line. The radius ( $r$ ) of circular radiating element defines the lower cut-off frequency for antenna's 10dB impedance bandwidth [30] as endorsed by HFSS simulation results shown in Fig.2 for different value of radius ( $r$ ) of circular disc radiating element. The lower cut-off frequency of antenna's 10dB bandwidth shifts from 1.766GHz to 2.258GHz when radius of circular disc is varied from 20mm to 14mm. The radius of circular radiating element is fixed to 20mm for our design in order to get lower frequency below 2GHz. A 3.5mm wide and 10mm deep rectangular groove has been placed exactly below the antenna feeding line to get extended 10dB input impedance bandwidth [31].



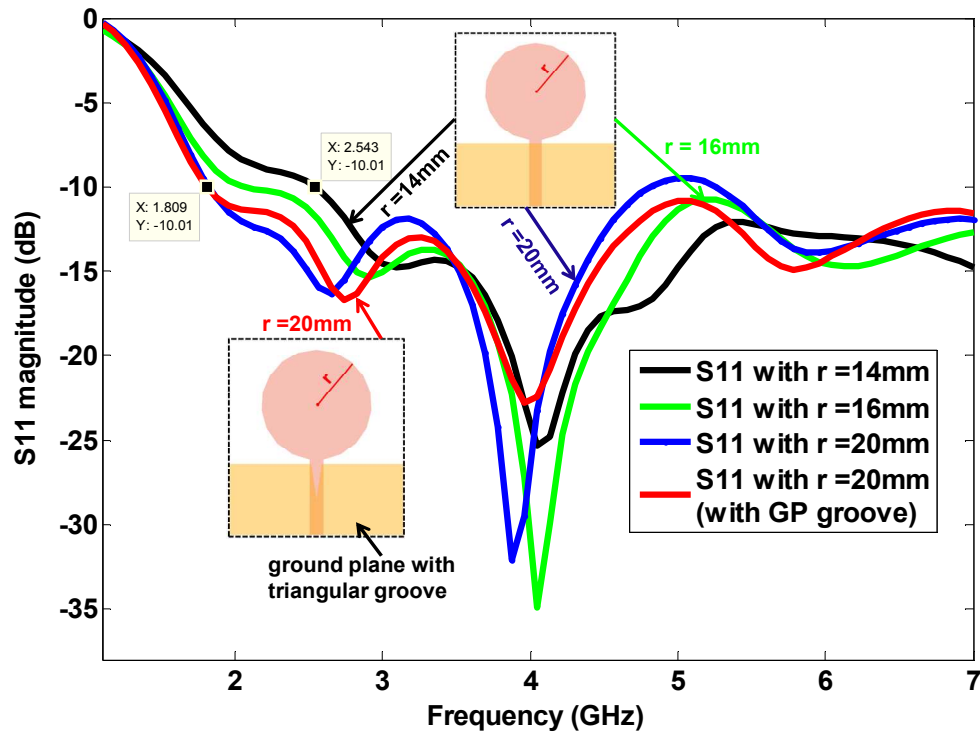


**Fig. 2.** Simulated S11 variations with different values of circular disc radius ( $r$ )

The size of partial ground plane ( $L_g$ ) also affects the impedance bandwidth of antenna in addition to spacing/gap between radiating element and ground plane. For our antenna, there is 1mm gap between ground plane and circular disc. Optimized ground plane dimensions are obtained by HFSS simulations for different values of ground plane's width ( $L_g$ ) as shown in Fig.3. For smaller values of  $L_g$ , input matching of antenna deteriorates around 3GHz but it improves at higher frequencies starting from 4GHz as clearly visible from Fig.3 for  $L_g=44$ mm. On the other hand, for larger values of  $L_g$ , antenna's matching degrades significantly in frequency range of 4-5GHz as clearly depicted for  $L_g=48$ mm. Thus, the optimized dimensions of partial ground plane are obtained as 19mmx44mm. The optimized antenna design has been implemented using 1.575mm thick RT/Duroid® 5880 substrate (with  $\epsilon=2.2$ , tangent loss =.001) as shown in Fig.1 with  $r=20$ mm and  $L_g=44$ .

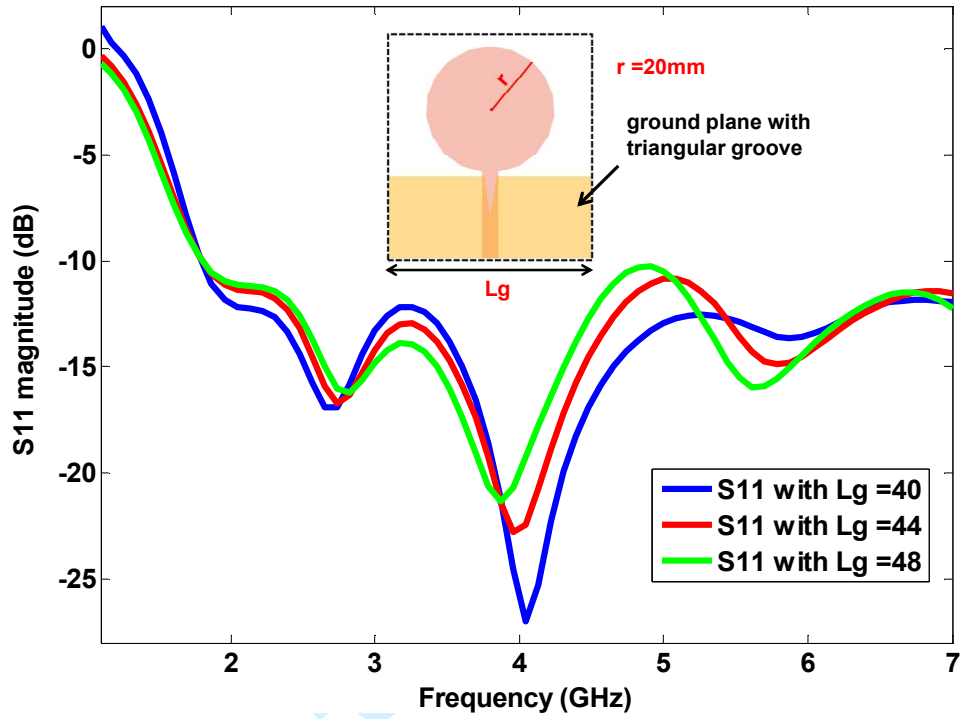


Fig. 3. Simulated S<sub>11</sub> for different values of ground plane width (L<sub>g</sub>)

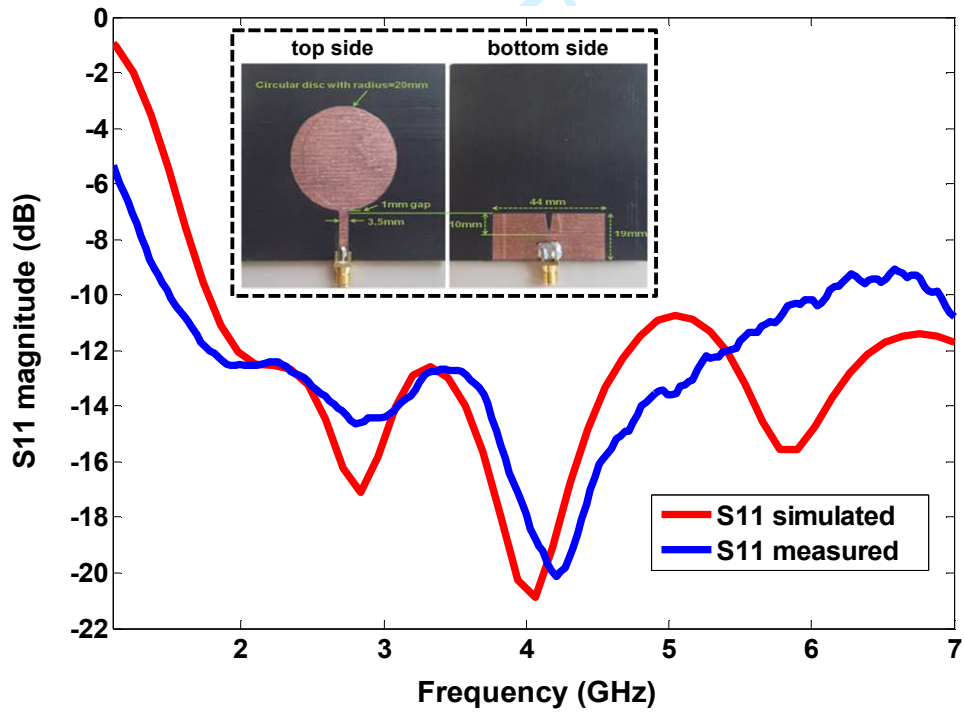


Fig. 4. Simulated vs. measured S<sub>11</sub> for implemented single port circular monopole antenna

HFSS simulation and measured input matching (S11) results for antenna implemented with optimized dimensions are shown in Fig.4. Measured 10dB impedance bandwidth for implemented single port circular disc antenna is 1.5GHz to 6GHz. HFSS simulated Peak Realized gain for Single port circular monopole antenna is also shown in Fig.5. The simulated gain varies between 3.5-6.6dBi in 2-6GHz frequency range.

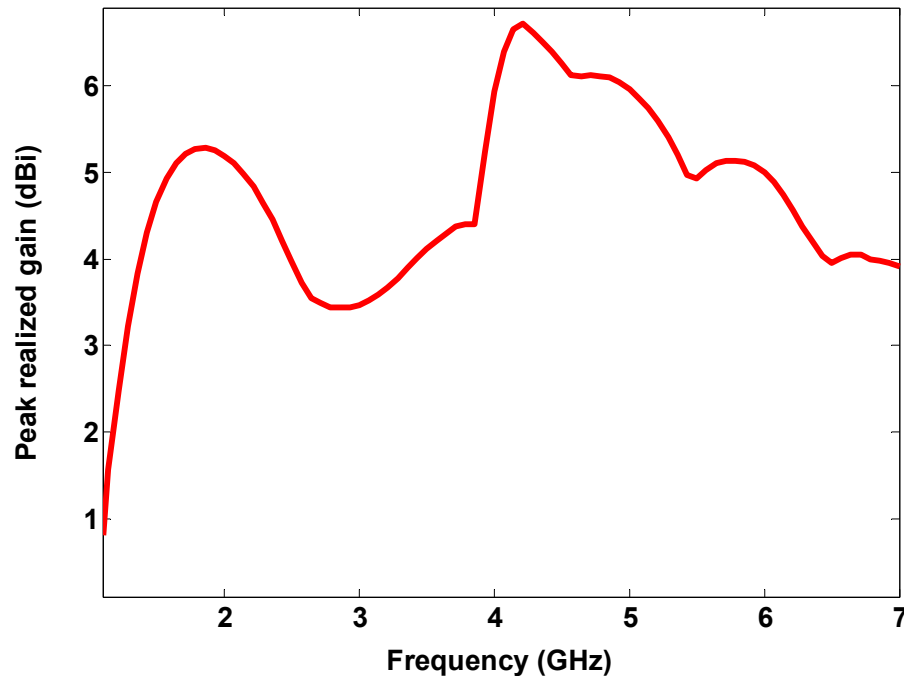
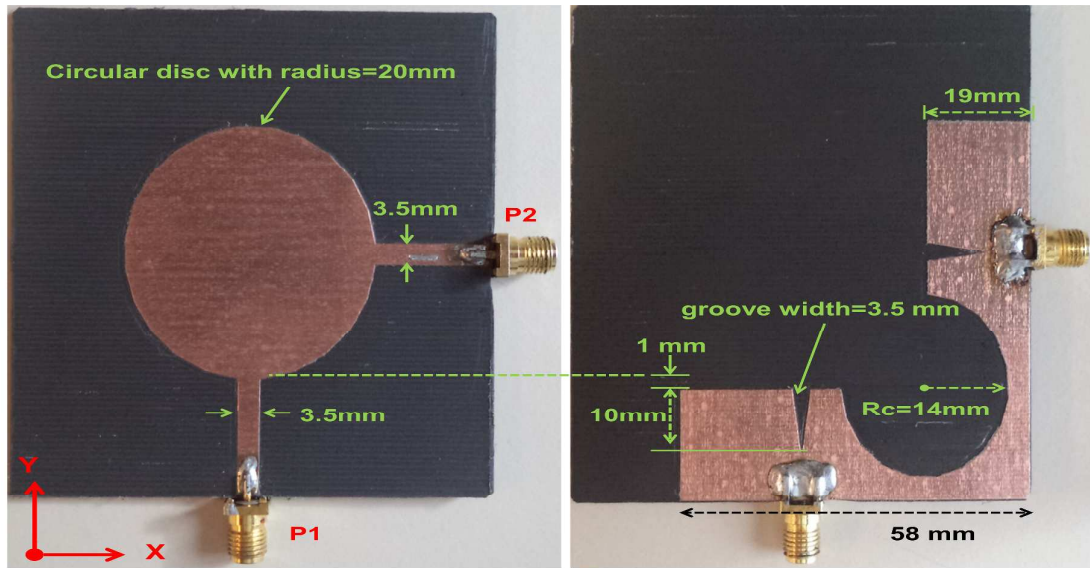


Fig. 5. HFSS simulated peak realized gain for single port circular monopole antenna

### 3. Dual port single element based circular disc monopole antenna

The dual port circular monopole antenna design is based on single port circular monopole antenna prototype as stated earlier. As shown in Fig.6, the radius of circular radiating element is 20mm with 3.5mm wide and 20mm long feed line to excite the radiating element from each port. There is 1mm gap between ground plane and radiating element. A 3.5mm wide and 10mm deep rectangular groove is again placed exactly below the each feeding line of antenna to get extended 10dB input impedance bandwidth as is the case with single port monopole antenna prototype.



**Fig. 6.** Dual port monopole antenna based on single circular disc element with circular cut of radius  $R_c$  in ground plane

Additionally, a circular cut of radius  $R_c$  in ground plane has been etched to obstruct the currents path between the two ports to enhance the interport isolation. As shown in Fig.7(b) by surface currents distributions, the mutual coupling is significantly reduced by circular cut etched in ground plane as compared to antenna structure without circular cut in ground plane shown in Fig.7 (a).

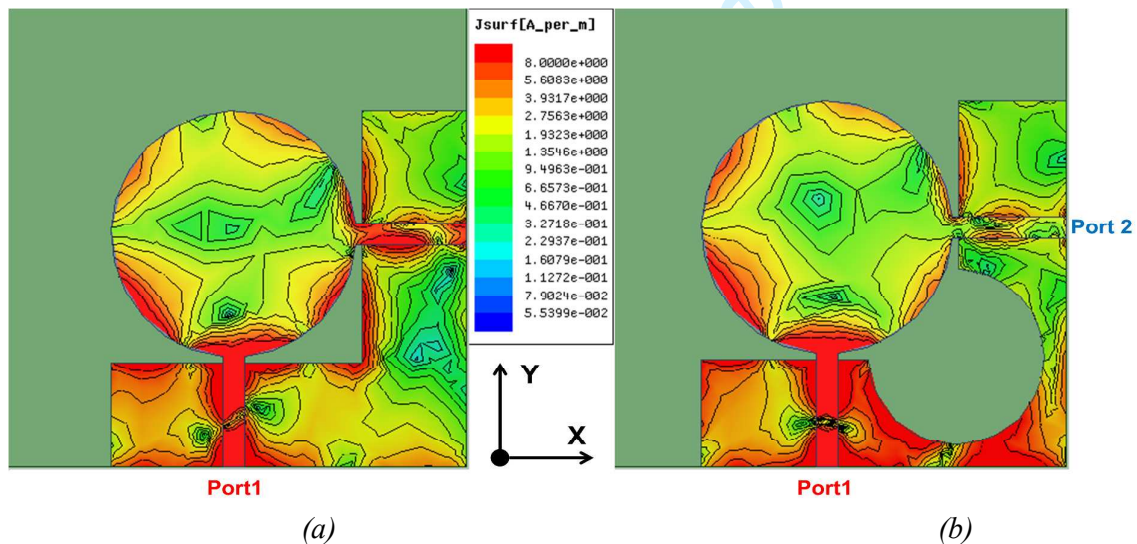


**Fig. 7.** Current distributions for proposed dual port circular disc antenna at 6GHz with port 1 excitation (a) without circular cut (b)with  $R_c=14\text{mm}$  circular cut in ground plane

The dimensions of ground plan slot ( $R_c$ ) have been optimized by HFSS simulations to achieve improved port to port isolation ( $S_{12}$ ) along with good antenna matching ( $S_{11}, S_{22}$ ) for 2-6GHz operating frequency. HFSS S-Parameters simulation results for different values of  $R_c$  are shown in Fig.8. For smaller slot dimensions, both antenna matching and interport isolation is degraded near 3.5GHz as shown in Fig.8 for 12mm radius of circular slot. On the other hand for larger dimensions of slot in ground plane, the antenna matching and interport isolation degrades around 6GHz frequency as shown in Fig.8 for the case of  $R_c=16$ mm. This is due to reduced ground plane size as already discussed for single port antenna. Although port to port isolation for this case is improved but the upper 10dB cut-off frequency is below 6GHz which is not acceptable for our required design. The circular slot with radius  $R_c=14$ mm has been selected as optimized value for our implemented antenna as it achieves 2-6GHz 10dB antenna input impedance and interport isolation is better than 15dB for this case.

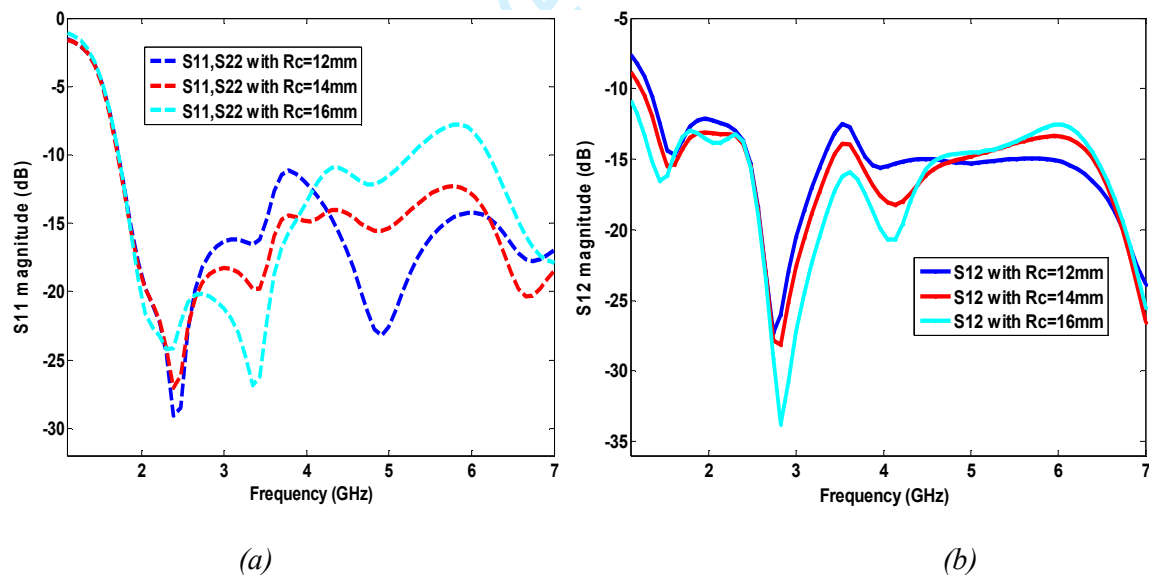


**Fig. 8.** HFSS simulation results for (a)  $S_{11}$ ,  $S_{22}$  with different radius( $R_c$ ) of circular cut in ground plane (b)  $S_{12}$  with different radius( $R_c$ ) of circular cut in ground plane

HFSS simulated peak realized gain for dual port circular disc monopole antenna is shown in Fig.9 for one port excitation and will be same for other port due to symmetrical

feeding structure at both ports . The antenna gain varies between 3.2-6.1dBi in 2-6GHz operating frequency range.

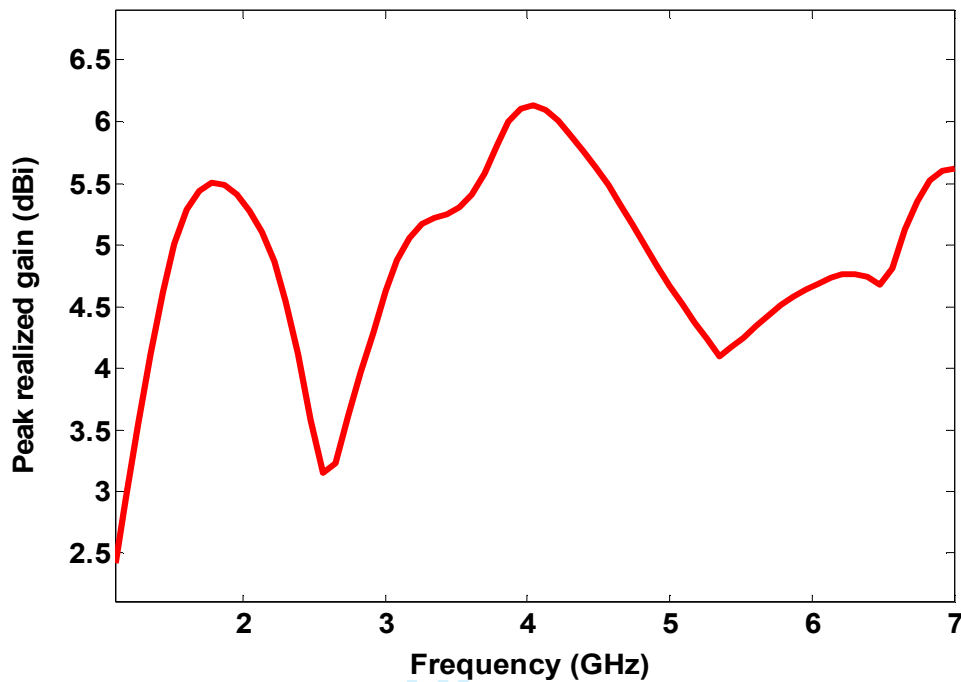


**Fig. 9.** HFSS simulated peak realized gain for dual port single element circular monopole antenna

#### 4. Test and measurement results for dual port circular disc monopole antenna

Implemented dual port circular disc antenna with optimized antenna and ground plane dimensions is printed on 1.575mm thick RT5880 substrate (with  $\epsilon=2.2$ , tangent loss =.001) as shown in Fig.6 with  $R_c=14$ mm. HFSS simulation and measured  $S_{11}$ ,  $S_{22}$  and  $S_{12}$  results for implemented antenna are shown in Fig.10. The measured 10dB lower cut-off frequency of impedance bandwidth for each port starts from 1.7GHz and upper cut-off frequency extends to more than 7GHz upper cut-off frequency as clearly indicated in Fig.10 as 10dB impedance band width. Implemented dual port circular disc antenna provides around 15dB port to port isolation for 1.7-7GHz as marked by green dotted line on Fig.10. Thus, the compact implemented dual port antenna based on single circular disc radiator provides a good interport RF isolation over wide range of frequencies.

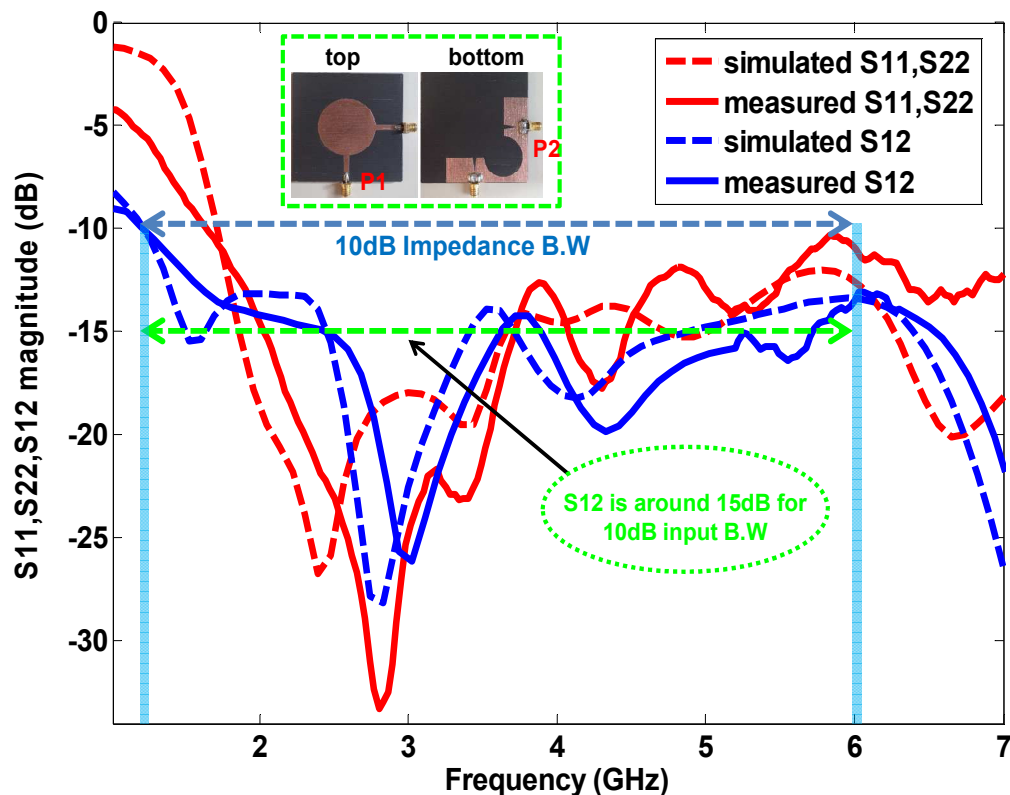


**Fig. 10.** Simulated vs. measured S-Parameters for dual port circular disc monopole antenna printed on 1.575mm thick RT5880 substrate

Simulated and measured E-plane and H-plane gain patterns for implemented antenna at 3GHz, 4GHz, 5GHz and 6GHz frequencies are shown in Fig.11 for port 2(P<sub>2</sub>) excitation. Port 1 and Port 2 are along y-axis and x-axis respectively. Therefore for port 1 YZ and XZ represent E-plane and H-plane respectively while for port 2 XZ is E-Plane and YZ is H-plane respectively. The antenna deploys same feeding structure to excite the radiating element from other port and measured input matching for second port has also similar characteristics as clear from Fig.10 so excitation from other port will provide similar but orthogonal radiation patterns. Hence due to symmetry of ports, simulated and measured E-plane and H-plane gain patterns for implemented antenna are sketched only for one port (i.e. port2).

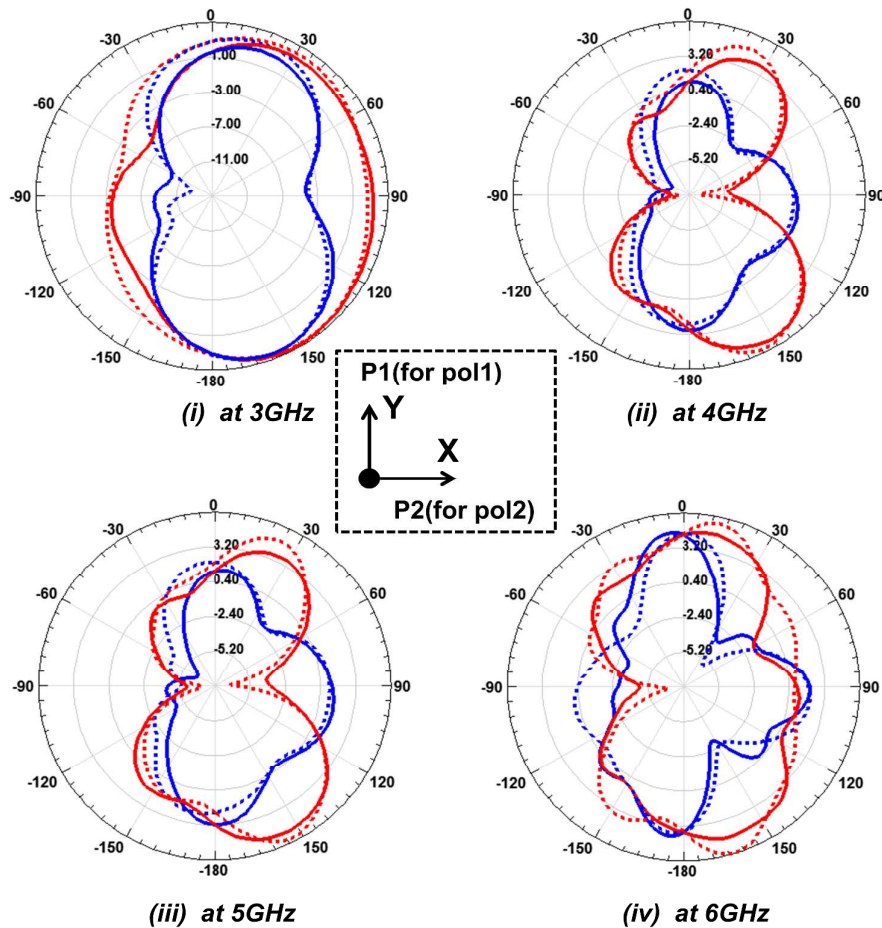


**Fig. 11.** Simulated (dotted lines) vs. measured (solid lines) E-Plane (red lines) and H-plane (blue lines) gain patterns of dual port antenna at 3GHz, 4GHz, 5GHz and 6GHz for port 1 excitation

Envelope correlation coefficient is another metric or indicator for performance evaluation of multiport antennas used for MIMO applications. The value of envelope correlation coefficient for multiport antennas should be as low as possible to ensure minimum port to port mutual coupling for MIMO antenna operation. Envelope correlation coefficient can be directly determined from far-field patterns but it can be computed using S-parameters results using equation (1) as given in [32]:

$$|\rho_e| = \frac{|s_{11}^* s_{12} + s_{21}^* s_{22}|^2}{(1 - (|s_{11}|^2 + |s_{21}|^2)) (1 - (|s_{22}|^2 + |s_{12}|^2))} \quad (1)$$



The acceptable antenna's envelope correlation coefficient for reliable MIMO performance is reported to be  $<0.5$  [9].

Simulated and measured correlation coefficients computed by simulated and measured S-parameters respectively are shown in Fig. 12. The measured value of envelope correlation coefficient for our antenna is less than 0.02 over required impedance bandwidth which ensures that implemented dual port antenna can be effectively used for MIMO applications over 2-6GHz frequency range.

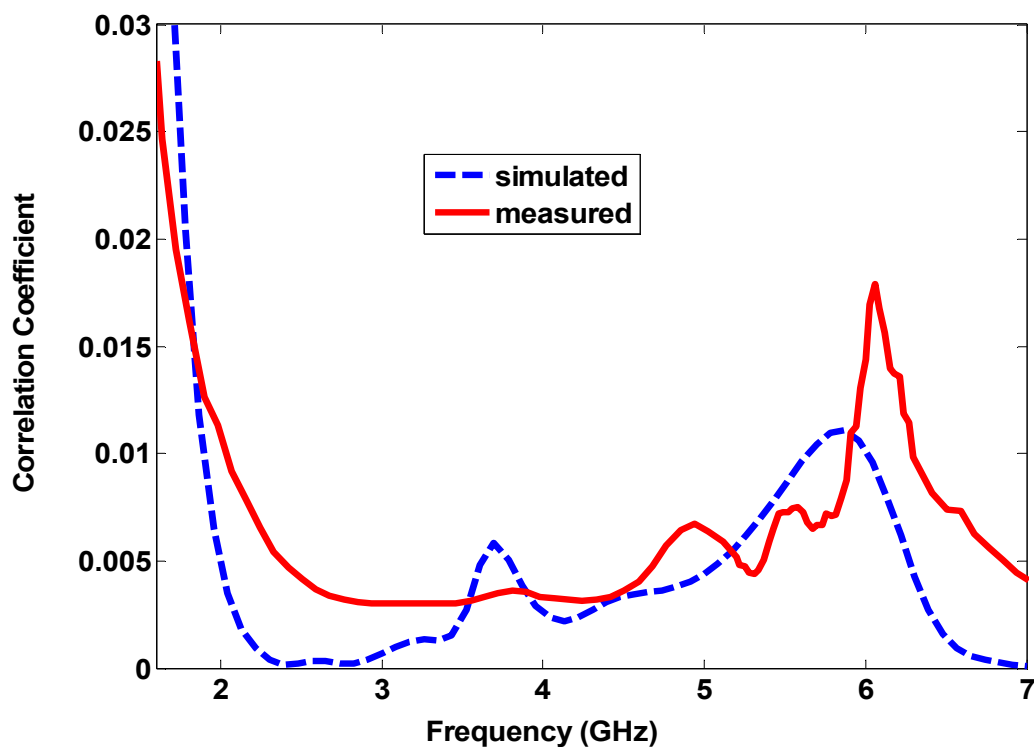


Fig. 12. Simulated and measured correlation coefficient for dual port single element monopole antenna

## 5. Conclusion

A compact (64mmx64mm) dual port monopole antenna based on single circular disc radiating element has been proposed and implemented for 2-6GHz MIMO applications. Implemented antenna provides more than 15dB port to port RF isolation in target 10-dB impedance bandwidth of 2-6GHz along with good radiation characteristics. Measured and

1  
2  
3 simulated S- parameter, gain patterns and correlation coefficients results are in good  
4  
5 agreement for proposed and implemented antenna. The implemented dual port antenna can be  
6  
7 effectively used for 2-6GHz MIMO applications based on its nice interport isolation which  
8  
9 was also endorsed by correlation coefficients computed by measured S-parameters.  
10

## 11 12 **Acknowledgments**

13  
14  
15 This work was supported in part by The Scientific and Technological Research Council  
16  
17 of Turkey (TUBITAK) under Grant 114E494.  
18

## 19 20 **References**

- 21  
22 [1] L. Malviya, R. K. Panigrahi, and M. V. Kartikeyan, "A 2×2 dual-band MIMO antenna with  
23 polarization diversity for wireless applications," *Progress In Electromagnetics Research C*, Vol.  
24 61, 91-103, 2016.  
25  
26 [2] G. J. Foschini and J. Gans, "On Limits of Wireless Communications in a Fading Environment  
27 when Using Multiple Antennas", *Bell Labs Technical Journal*, vol. 1, no. 2, Lucent Technologies,  
28 pp 41- 59, 1996.  
29  
30 [3] H. Sampath, S. Talwar, J. Tellado, V. Erceg, and A. Paulraj, "A fourth- generation MIMO-OFDM  
31 broadband wireless system: Design, performance, and field trial results, " *IEEE Commun. Mag.*,  
32 vol. 40, no. 9, pp. 143-149, 2002.  
33  
34 [4] Jayasooriya, C.K.K., Kwon, H.M., Bae, S., et al.: 'Miniaturized circular antennas for MIMO  
35 communication systems- pattern diversity'. *Int. ITG Workshop on Smart Antennas*, 2010, pp.  
36 331–334  
37  
38 [5] S. B. Sahay, K. C. Bhagwat and P. R. J. Mohan, "Exploitation of MIMO techniques for reliable  
39 HF communication," *2012 International Conference on Signal Processing and Communications*  
40 *(SPCOM)*, Bangalore, 2012, pp. 1-4.  
41  
42 [6] K. Pachori and A. Mishra, "Performance analysis of MIMO systems under multipath fading  
43 channels using linear equalization techniques," *International Conference on Advances in*  
44 *Computing, Communications and Informatics (ICACCI)*, 2015, Kochi, 2015, pp. 190-193.  
45  
46 [7] Minz, L., Garg, R.: 'Reduction of mutual coupling between closely spaced PIFAs', *Electron.*  
47 *Letters*, 2010, 46, (6), pp. 392–394  
48  
49 [8] Park, J., Choi, J., Park, J.-Y., et al.: 'Study of a T-shaped slot with a capacitor for high isolation  
50 between MIMO antennas', *IEEE Antennas Wirel. Propagation Letters*, 2012, 11, pp. 1541–1544  
51  
52 [9] K. Chung, J. H. Yoon, "Integrated MIMO Antenna with High Isolation Characteristic" *Electron.*  
53 *Letters*, vol. 43, pp. 199-201, 2007.  
54  
55  
56  
57  
58  
59  
60

- 1  
2  
3 [10] T.Y. Wu, S.T. Fang and K.L. Wong, "Printed diversity monopole antenna for WLAN operation,"  
4 Electron. Letters, 38, (25), pp. 1625–1626, 2002.  
5  
6 [11] C. Jae-Young, et al., "Low correlation MIMO antenna for LTE 700MHz band," in Antennas and  
7 Propagation (APSURSI), 2011 IEEE International Symposium on 2011, pp. 2202-2204.  
8  
9 [12] L. Liu, S. W. Cheung and T. I. Yuk, "Compact MIMO Antenna for Portable Devices in UWB  
10 Applications," in *IEEE Transactions on Antennas and Propagation*, vol. 61, no. 8, pp. 4257-4264,  
11 Aug. 2013.  
12  
13 [13] Li, H., Xiong, J., Ying, Z., et al.: 'Compact and low profile co-located MIMO antenna structure  
14 with polarization diversity and high port isolation', Electron. Letters, 2010, 46, (2), pp. 108–110  
15  
16 [14] S. Soltani and R. D. Murch, "A Compact Planar Printed MIMO Antenna Design," in *IEEE*  
17 *Transactions on Antennas and Propagation*, vol. 63, no. 3, pp. 1140-1149, March 2015.  
18  
19 [15] A. Toktas and A. Akdagli, "Compact multiple-input multiple-output antenna with low correlation  
20 for ultra-wide-band applications," in *IET Microwaves, Antennas & Propagation*, vol. 9, no. 8, pp.  
21 822-829, 2015.  
22  
23 [16] C. H. See, R. A. Abd-Alhameed, Z. Z. Abidin, N. J. McEwan and P. S. Excell, "Wideband  
24 Printed MIMO/Diversity Monopole Antenna for WiFi/WiMAX Applications," in *IEEE*  
25 *Transactions on Antennas and Propagation*, vol. 60, no. 4, pp. 2028-2035, April 2012.  
26  
27 [17] X. S. Yang, L. Zhang, L. L. Zhou, R. Q. Wang and X. J. Li, "Planar two-element UWB MIMO  
28 antennas with high isolations," *IEEE International Conference on Computational*  
29 *Electromagnetics (ICCEM)*, Hong Kong, 2015, pp. 363-365  
30  
31 [18] C. M. Luo, J. S. Hong and L. L. Zhong, "Isolation Enhancement of a Very Compact UWB-  
32 MIMO Slot Antenna With Two Defected Ground Structures," in *IEEE Antennas and Wireless*  
33 *Propagation Letters*, vol. 14, no. , pp. 1766-1769, 2015  
34  
35 [19] M. S. Khan, A. D. Capobianco, A. Naqvi, B. Ijaz, S. Asif and B. D. Braaten, "Planar, compact  
36 ultra-wideband polarization diversity antenna array," in *IET Microwaves, Antennas &*  
37 *Propagation*, vol. 9, no. 15, pp. 1761-1768, 12 10 2015  
38  
39 [20] Chen, S.C., and Wang, Y.S.: 'A decoupling technique for increasing the port isolation between  
40 two strongly coupled antennas', *IEEE Transactions on Antennas Propagation* , 2008, 56, pp.  
41 3650–3658  
42  
43 [21] Xian, Q., Hui, L.W., and Sailing, H.: 'A decoupling technique for increasing the port isolation  
44 between two closely packed antennas'. *Antennas and Propagation Society Int. Symp.*, Chicago,  
45 IL, USA, July2012, pp. 1–2  
46  
47 [22] Skycross, Inc, iMAT Antenna Whitepaper, January 2008, <http://www.skycross.com/>.  
48  
49 [23] N.K. Kiem, D.N. Dinh, H.T. Viet, & D.N. Chien, "A novel design of dual-feed single-element  
50 antenna for 4G MIMO terminals", *Progress in Electromagnetics Research Symposium*, pp. 1827,  
51 2012.  
52  
53  
54  
55  
56  
57  
58  
59  
60

- 1  
2  
3 [24] F. M. Caimi, and M. Montgomery, "Dual feed, single element antenna for WiMAX MIMO  
4 application," *International Journal of Antennas and Propagation*, Vol. 2008, Article ID 219838, 5  
5 pages, 2008.  
6  
7 [25] T. Aboufoul, A. Alomainy and C. Parini, "A planar dual fed UWB monopole antenna with  
8 polarization diversity for cognitive radio sensing," *Antennas and Propagation Conference*  
9 *(LAPC), 2012 Loughborough*, Loughborough, 2012, pp. 1-4.  
10  
11 [26] Moradikordalivand, Alishir, et al. "Dual polarized MIMO antenna system for WiFi and LTE  
12 wireless access point applications." *International Journal of Communication Systems* (2014)  
13  
14 [27] Nawaz, H. and Tekin, I., "Dual port single patch antenna with high interport isolation for 2.4 GHz  
15 in-band full duplex wireless applications". *Microw. Opt. Technol. Lett.*, 58: 1756–1759.  
16 doi: 10.1002/mop.29899, 2016  
17  
18 [28] K. P. Ray, "Design Aspects of Printed Monopole Antennas for Ultra-Wide Band Applications,"  
19 *International Journal of Antennas and Propagation*, vol. 2008, Article ID 713858, 8 pages, 2008.  
20 doi:10.1155/2008/713858  
21  
22 [29] N. P. Agrawal, G. Kumar and K. P. Ray, "Wide-band planar monopole antennas," in *IEEE*  
23 *Transactions on Antennas and Propagation*, vol. 46, no. 2, pp. 294-295, Feb 1998.  
24  
25 [30] Jianxin Liang, C. C. Chiau, Xiaodong Chen and C. G. Parini, "Study of a printed circular disc  
26 monopole antenna for UWB systems," in *IEEE Transactions on Antennas and Propagation*, vol.  
27 53, no. 11, pp. 3500-3504, Nov. 2005.  
28  
29 [31] Gilliard N. Malheiros-Silveira, Ricardo T. Yoshioka, Jose E. Bertuzzo, and Hugo E. Hernandez-  
30 Figueroa, "Printed monopole antenna with triangular-shape groove at ground plane for blue-tooth  
31 and UWB applications," *Microwave and Optical Technology Letters*, vol. 57, no. 1, pp. 28–31,  
32 2014.  
33  
34 [32] S. Blanch, J. Romeu, and I. Corbella, "Exact representation of antenna system diversity  
35 performance from input parameter description," *Electronics Letters*, vol. 39, no. 9, pp. 705–707,  
36 2003.  
37  
38  
39  
40  
41  
42  
43  
44  
45  
46  
47  
48  
49  
50  
51  
52  
53  
54  
55  
56  
57  
58  
59  
60